

Oblique Impact Study in Thin Steel Armour Plate

S.N. Dikshit

Defence Metallurgical Research Laboratory, Hyderabad - 500 058.

ABSTRACT

Results of a study on the performance of 10 mm low alloy, rolled-homogeneous armour (RHA) plate when impacted by 20 mm diameter steel ogive-shaped projectile at 15, 30 and 45° angles of attack in the subordnance velocity regime are presented. Experimental results show that 10 mm steel plate provides full protection at 45° obliquity up to a striking velocity of 530 m/s. At low velocity ($V < 350$ m/s), the plate provides protection at 30° obliquity, but fails to provide protection at an angle of attack of 15°, even at low velocity ($V = 300$ m/s). It is also observed that normal component of the striking velocity of the projectile is the main cause of plate perforation.

1. INTRODUCTION

Most of the projectile-target interaction studies relate to the normal impact and only a few workers have carried out analysis at oblique angles of impact. Further, limited experimental data is available on the oblique impact interactions of the projectile and the target¹. The reason for the nonavailability of experimental data is linked to the fact that military fighting vehicles are designed with sloped armour. Additionally, analysis of an oblique impact event is quite complex due to the introduction of additional turning and bending stresses on the impacting projectiles. However, analytical equations have been developed to predict residual velocity of the projectile² and also the influence of obliquity on plate performance³. Velocity-drop experiments conducted⁴ at 300 m/s and⁵ 400 m/s showed significant differences in the findings of the two investigators and the results exhibited a large degree of scatter¹. These investigators used Al/steel targets which were impacted by lead bullets⁴ and hard steel projectiles

of cylindro-conical and cylindrical shapes. The nature of energy absorbed during the oblique impact of a hard ball onto a semi-infinite ductile target material is found to be a strong function of both the impact velocity and the impact angle⁶. In this investigation, armour grade steel plate and ogive-shaped steel projectile having strengths higher than that of the target plate have been used.

The aim of this investigation was to ascertain the protective capability (ballistic performance) of 10 mm steel armour plate when impacted by ogive-shaped steel projectile of 20 mm diameter at different obliquities and in the subordnance velocity regime ($V < 1000$ m/s).

2. EXPERIMENTAL DETAILS

2.1 Procedure

A low alloy rolled-homogeneous armour (RHA) steel plate of 10 mm thickness was used as the target. The plates were used in the as-received condition. Hardness of the plates, as measured on

Vicker's scale, was 370 ± 10 Hv. The Charpy V notch impact value was 45 J (25°C).

A steel projectile of 20 mm diameter with ogive shape and length-to-diameter ratio of 5.73 was impacted on the target at 15, 30 and 45° obliquities. Projectile hardness was 600 Hv and mass was 110 g. The plate-projectile combination selected represents plane stress condition (unconstrained plastic flow) where bulging of the target plate is visualised at all velocities of the projectile.

The RHA plates of 10 mm thickness and 450 x 300 mm size were mounted on the firing stand which was designed to provide 15, 30 and 45° angles of attack. Plates were firmly clamped on to the firing stand, although the degree of clamping does not have a significant effect on ballistic performance of the armour plate⁷. Change in velocity was achieved by changing the charge mass. Velocity of the projectile was measured using foil technique⁸. The projectile was fired from a rifled gun. Four to six rounds were impacted on each plate. Distance between the craters was ensured to be more than three times the diameter of the projectile. At 15° obliquity, only two rounds could be impacted and it was not feasible to get the striking velocity of the projectile below 300 m/s due to technical and safety reasons.

2.2. Experimental Parameters

After the ballistic tests, each impact-crater was subjected to detailed examination. First, the impact craters on the target plate were photographed on both entry and exit sides. Depth of penetration (X_p) for all the craters on each plate was measured using a portable stand having 4-point support, fabricated for this purpose (Fig. 1). In case of bulge formation, X_p included thickness of the plate and depth of the bulge so formed by the penetrating projectile. Crater volume (U) was determined by filling the craters, up to the original target plate level, with plasticine of known density. Crater length (D_a), crater width (D_b) and bulge height (H_b) i.e., height of the bulge formed on the back-face of the plate,

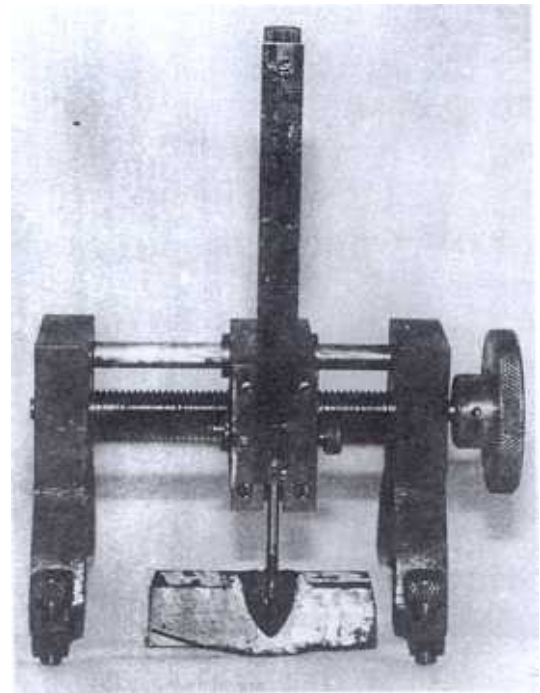


Figure 1. Portable four-point support device for measuring depth of penetration, bulge height, bulge length and bulge width.

were also measured using a portable stand. The experimental parameters studied in this investigation are depicted in Fig. 2, wherein the processes of bulging, stretching, partial penetration and perforation are explained.

3. EXPERIMENTAL RESULTS

3.1 Plate Damage Studies

The steel armour plates impacted at 15, 30 and 45° obliquities were examined for assessing the nature and mode of deformation of the plate material during projectile penetration. Back-face effects on these plates are presented in Table 1. From Table 1, it is observed that there is no plate perforation even at the highest velocity ($V \sim 530$ m/s) at 45° obliquity, whereas perforation occurs even at the lowest velocity ($V \sim 300$ m/s) at 15° obliquity. At 30° obliquity and at a velocity of 370 m/s, the plate failed to provide protection against 20 mm steel projectile due to the development of multiple wide cracks on the bulged surface.

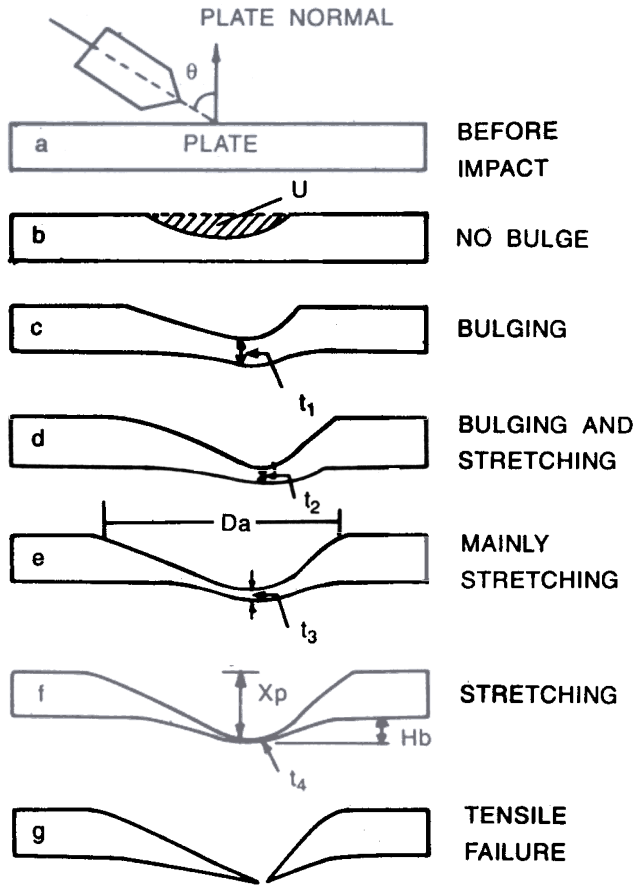


Figure 2. Parameters studied in oblique impact situation

Typical exit locations in 10 mm plate impacted at 15° angle of attack are shown in Fig. 3. Figure 3(a) shows the rear-face of the plate impacted at low velocity ($V = 300$ m/s). At a velocity of 340 m/s, complex perforation is noticed in Fig 3(b). Predominant star-shaped tensile failure of 10 mm plate, without perforation, is observed at 30° angle of attack at a striking velocity of 340 m/s. The plate is, however, perforated completely at a velocity of 430 m/s (Fig. 4). Figure 5 shows the front and back-face of 10 mm plate impacted at an angle of attack of 45° and at a velocity of 530 m/s. Initiation of crack in the bulged region is clearly visible in Fig. 5(b) and there is no perforation of the plate. Formation of lip on the front-face of the plate is also not evident in Fig. 5(a).

3.2 Penetration Depth & Volume

The depth up to which the projectile penetrates (X_p) into the steel plate and the volume of the crater

Table 1. Nature of damage on the back-face

Obliquity (°)	Velocity (m/s)	Observations
45°	290 (R), NL	Fine bulge
	350 (R), NL	Bulge commenced
	380 (R), NL	Smooth, bigger bulge without crack
	430 (R), NL	Smooth, bigger bulge without crack
	470 (R), NL	Smooth bulge without crack
30°	530 (R), NL	Smooth, large bulge with small crack
	300 (R), NL	Smooth bulge without crack
	340 (R), NL	Smooth bulge with star-shaped crack
	370 (R), NL	Smooth bulge with wide crack
	430 (NR),NL	Complete perforation in the bulged surface
15°	300 (NR),NL	Bulge with wide crack
	340 (NR),NL	Partial perforation with wide, multi cracks on the bulge

NR-No ricochet, R-Ricochet, NL-No lip formed on front-face

(U) created in the process were experimentally measured over a range of impact velocities at 15, 30 and 45° angles of attack on 10 mm thick plates. The results are presented in Fig. 6.

Comparison of data on X_p given in Fig. 6(a) at 15, 30 and 45° angles of attack indicates that even at lowest velocity of impact ($V=300$ m/s), magnitude of X_p at 15° exceeded the total thickness of the target plate. The magnitude of X_p at 30° ($V = 300$ m/s) has attained a value just equal to the thickness of the 10 mm plate, whereas at 45° ($V = 300$ m/s), the magnitude of X_p is about one third of the plate thickness. The target plate is completely perforated at a velocity of 340 m/s at an angle of attack of 15° (Fig. 3(b)), whereas in the case of 30° angle of attack, complete perforation takes place at a striking velocity of about 430 m/s (Fig. 4). At a velocity of 530 m/s and at an angle of attack of 45°, there is evidence of initiation of the fracture in the plate (Fig. 5). Volume of the crater created by the

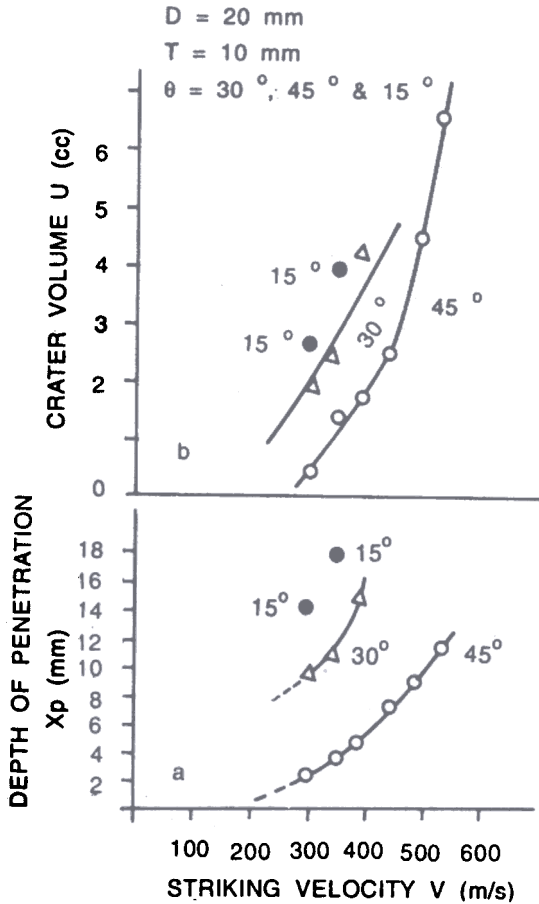


Figure 3. Typical appearance of back-face damage on 10 mm plate when impacted by 20 mm diameter steel projectile at 15° angle of attack, at striking velocities of (a) 300 m/s (b) 340 m/s.

impacting projectile on 10 mm thick plate at 15, 30 and 45° angles of attack shows a trend similar to X_p . Values of U and X_p are mainly governed by the strength of the projectile in relation to that of the target.

3.3. Crater Length & Width

Crater length (D_a) and crater width (D_b) as shown in Fig. 2 were measured using a portable stand. D_a and D_b basically represent the major and the minor axes of the crater formed on the target plate under oblique condition. Figure 7 shows variation in length-to-width (D_a/D_b) ratio of craters with striking velocity of the projectile. Crater length-to-width ratio is plotted for 30 and 45° angles of attack. Slope of D_a/D_b at 30° obliquity, in Fig. 7, is higher than that at 45° obliquity.

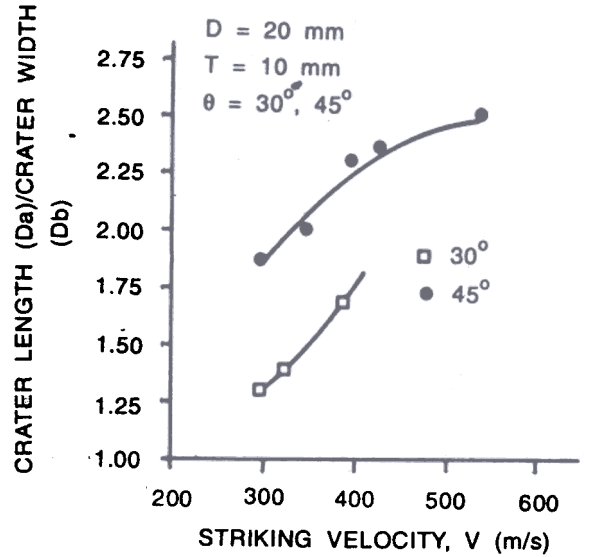


Figure 4. Typical appearance of back-face damage on 10 mm plate at 30° angle of attack and at a striking velocity of 430 m/s.

3.4. Bulge Height

Bulge height (H_b) (Fig. 2(c)), was measured on a 10 mm plate impacted at 45° angle of attack. Figure 8 shows variation in H_b with striking velocity of the projectile for an impact of 45° At

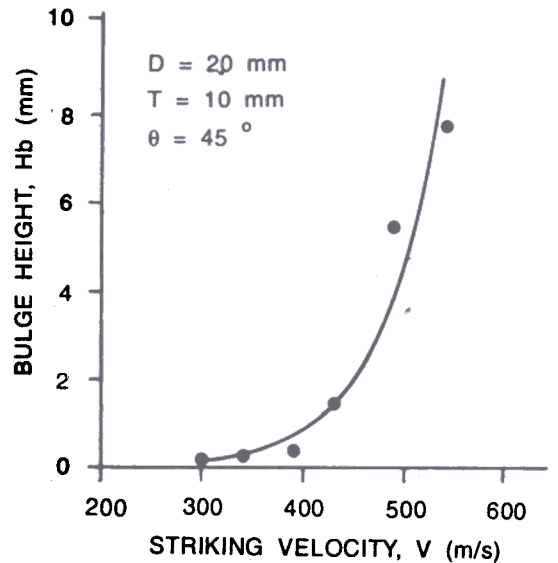


Figure 5. Typical appearance of crater formed on (a) front-face and (b) back-face of 10 mm plate after an impact at 45° by 20 mm diameter steel projectile at a velocity of 530 m/s.

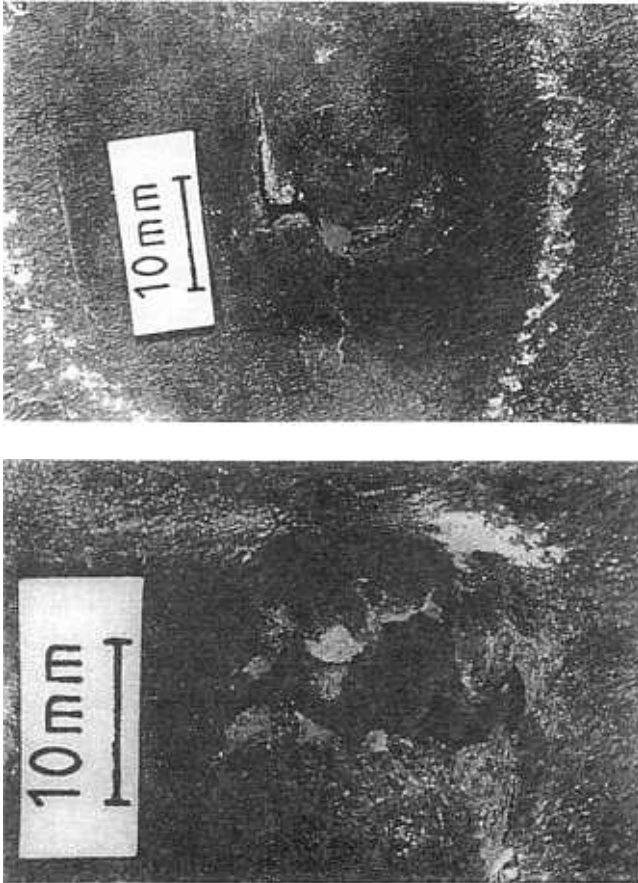


Figure 6. Variation in (a) depth of penetration and (b) crater volume with striking velocity of 20 mm projectile, for 15, 30 and 45° angles of attack.

15 and 30° angles of attack, H_b could not be measured due to perforation of the plate in the bulged region.

4. DISCUSSION

4.1 Ballistic Behaviour

Figure 6 provides evidence for the protective ability of 10 mm plate when impacted by a 20 mm diameter steel projectile. The 10 mm plate impacted at 45° angle of attack by a 20 mm diameter steel projectile is capable of providing full protection even at a striking velocity of 530 m/s. Considering X_p and examining the back-face effects, it is clear that 10 mm plate gets damaged by a 20 mm diameter projectile even at very low velocity ($V=300$ m/s) at



Figure 7. Variation in crater length-to-width, with striking velocity at 30 and 45° angles of attack by 20 mm diameter steel projectile.

an angle of attack of 15°. However, at 30° angle of attack, the plate provides protection up to a striking velocity of 340 m/s, but major cracks are developed on the bulged surface at a velocity of 370 m/s. A bulge with a major crack or perforation is considered as an indication of plate failure, in view of the protection considerations. A large and smooth bulge with minor crack is not considered to be plate failure. The variation in X_p with obliquity (θ) is shown in Fig. 7. As expected, X_p decreases with increasing obliquity. This kind of ballistic behaviour of steel armour plate is suggestive of the use of sloped armour plates in the design of an armoured fighting vehicle so as to minimise the weight-penalty.

4.2 Crater Size

With increasing velocity, D_a/D_b ratio increases at both 30° and 45° angles of attack. Increase in this ratio is more dramatic at 45° than that at 30° angle of attack; this is due to increase in D_a at 45° obliquity. Increased D_a is associated with increased horizontal component and decreased normal component of the projectile velocity. Also, the nature of increase in both the cases is different. Best-fit-polynomial approximation was used to correlate the striking velocity (V) and D_a/D_b ratio and the following polynomials were obtained:

$$D_a / D_b = .48148 \times 10^{-5} V^2 - 0.00599 V + 1.767 \quad (2)$$

$$D_a / D_b = -0.91952 \times 10^{-6} V^2 + 0.0103 V - 0.4207 \quad (3)$$

Equations (2) and (3) correspond to 30° and 45° angles of attack, respectively. Digging tendency of the projectile into the plate material at 30° angle of attack, especially at a higher velocity, is the cause of the higher slope at 30° (Fig. 7). This aspect gets further clarified on comparing the shape of the craters shown in Figs 4 and 5. It can thus be safely concluded that the severity of the angle of attack at 30° is quite high and the armour designer should avoid this kind of slanting of the armour plates.

4.3 Bulge Profile

Increase in bulge height H_b at low velocity ($V = 300-400$ m/s) is quite small. However, increase in H_b is quite abrupt beyond a striking velocity of 425 m/s. This abrupt increase in the value of H_b at higher striking velocity is due to bending and stretching⁸ of the bulge formed at the back-face of the 10 mm plate. H_b as shown in Fig. 8, increases exponentially with increase in striking velocity of the projectile and these are related as per the following expression:

$$H_b = 0.00105 \exp (0.0168 V) \quad (4)$$

Initial part of the curve in Fig. 8, up to the striking velocity of 425 m/s, can thus be termed as the zone of bending and the later part pertaining to

higher velocity ($V > 425$ m/s) can be termed as the zone of stretching. It is observed that during the zone of bending, there is little or no stretching of the bulged material and the main source of energy absorption is only through bending of the plate. However, in the zone of stretching, there may be bending, but the main source of energy absorption is by way of stretching of the bulged material at high velocities⁸. The term stretching is used here to indicate progressive reduction in the thickness ($t_4 < t_3 < t_2 < t_1$) of the material in the bulged region, ahead of the penetrating projectile (Figs 2 (c-g)). Once the stretching reaches a critical stage, tensile failure occurs in the bulged region (Fig. 2 (g)). Tensile failure may also be associated with shearing of the plate material in contact with the tip of the projectile.

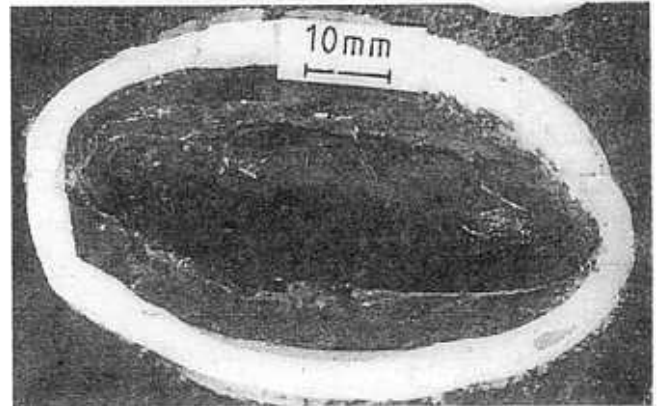


Figure 8. Variation in bulge height with striking velocity at 45° angle of attack.

4.4 Normal Component & Obliquity

The normal component of the striking velocity in an oblique condition can be represented as $V \cos \theta$, where V is the striking velocity of the projectile on the target and θ is the angle of attack. As mentioned in Section 4.1, the large smooth bulge with a wider crack is considered to be an indication of plate failure with partial or complete perforation of the plate. Data on the striking velocity of the projectile, at different obliquities at which the plate is considered to have failed, are given in Table 1. It is seen that 10 mm thick steel armour plate gets damaged at 340, 430 and 530 m/s at 15° , 30° and 45° obliquities, respectively. The computed values of $530 \cos 45$, $430 \cos 30$ and $340 \cos 15$ are nearly the same, keeping in view the scatter of the velocity. It is thus observed that though striking velocities are different (at different obliquities, at which plate damage actually occurs), the normal component of these striking velocities has the same value. This observed fact leads to a conclusion that it is the normal component of the striking velocity which is responsible for X_p or plate damage.

The above-mentioned experimentally observed fact is actually related to the increased path length obtained at increased obliquity. This increased path length enhances the plastic deformation zone forming around the penetrating projectile in the process of penetration and or perforation³. Such a process will lead to more and more energy dissipation in the plate (E_{pl}) ensuring maximum loss of the projectile energy. Earlier investigators⁹ also observed that as the normal component of velocity decreases with increasing obliquity, the crater becomes elongated. Such an elongated crater is observed to be formed on the plate when impacted at 45° obliquity (Fig. 8). Formation of this kind of elongated crater at higher obliquity, having lesser depth of penetration, is mainly due to decreased normal component of the projectile velocity. On examination of the front-face of the impacted plate, it is noticed that as the plate

obliquity increases, craters tend to be semielliptical and elliptical in shape due to decreasing normal component of the projectile velocity. It can be further stated that at $\theta = 0^\circ$ (i.e. when the direction of the incoming projectile coincides with the normal of the plate), normal component of projectile velocity ($V \cos \theta$) attains maximum value and causes maximum penetration in the plate and the shape of the crater will be hemispherical. On the contrary if $\theta = 90^\circ$ (i.e. direction of motion of the projectile makes 90° angle with the normal of the plate), the normal component will be minimum and the projectile will travel parallel to the surface of the plate without penetrating the target plate (just what is called grazing). This again justifies the statement that it is the normal component of projectile velocity which causes maximum penetration and the target plate gets damaged. Variation of X_p with obliquity (Fig. 9) shows decreasing X_p with increasing obliquity (at a particular velocity of the projectile) due to increased path length and the accompanying energy

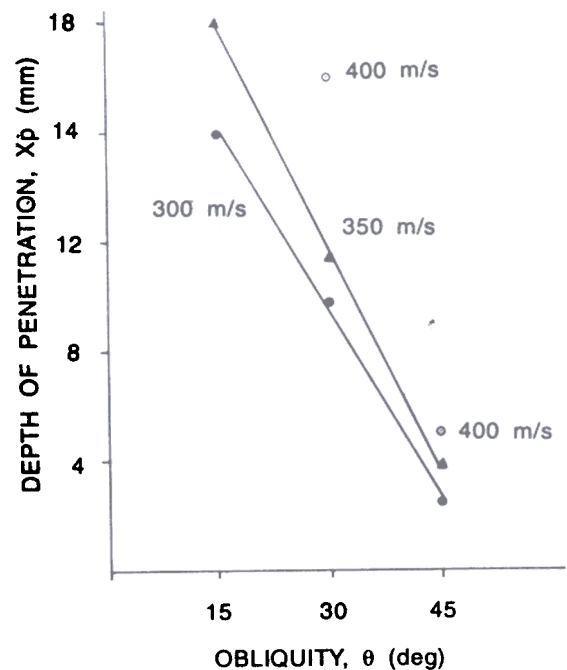


Figure 9. Variation in depth of penetration with obliquity at different velocities.

dissipation due to plastic flow of the target material³.

4.5 Energy Dissipation

Target thickness (T) to projectile diameter (D) ratio plays a vital role in deciding the nature and extent of damage to the target plate. It is mainly due to the fact that T/D ratio governs the constrained or unconstrained plastic flow of the target material ahead of the penetrating projectile. Projectile velocity, its nose shape and the target strength are other important parameters associated with the influence of T/D on the nature of damage. Nature and type of target damage in relation to T/D either being less than 1, equal to 1 or more than 1 has been studied¹⁰. Summary of the target behaviour on interaction with projectiles¹¹ is given in Table 2. Armour-grade steel target plates have not been used in these studies and hence accurate assessment of the protective capability of the steel armour plates is difficult to be made, especially at different obliquities.

The present investigation was aimed at ascertaining the ballistic performance of the thin steel armour plates (T/D being less than 1) when impacted by an ogive-shaped steel projectile at different obliquities in the subordnance velocity regime (velocity being < 1000 m/s.). The theoretical analysis has not been given in this investigation and the valid reasons for not offering have been given in the succeeding paras. At this stage, it would be pertinent to address the energy dissipation mode based on the experimental evidence. As mentioned in Section 3.1, the following experimental observations are made:

- (a) Crater formation (without lip formation on the front-face of the plate)
- (b) Plate bending
- (c) Plate bulging indicating unconstrained plastic flow
- (d) Plate stretching
- (e) Star-shaped tensile failure of the target material
- (f) Hole enlargement

- (g) Petal formation at the back-face of the plate (observed only at higher velocities, wherein projectile perforated the plate, also only 4-5 petals are formed)
- (h) Scabbing, fragmentation and radial fracture effects have not been noticed at any velocity and at any obliquity

In the light of the above observations and findings of a similar investigation available elsewhere⁸, the following energy balance can be presented:

$$KE_p = E_{pl} + E_{in} + E_{fric} + E_{bulge}$$

where

$$E_{bulge} = E_{ben} + E_{str}$$

Therefore,

$$KE_p = E_{pl} + E_{in} + E_{ben} + E_{str} + E_{fric}$$



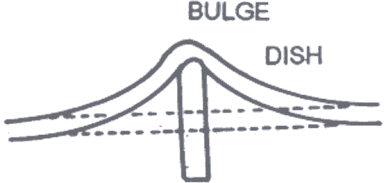

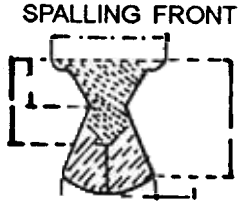
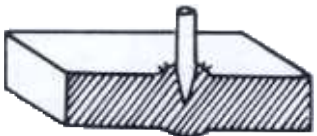
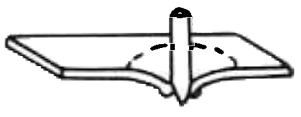

where

KE_p	Energy dissipated in the plate
E_{pl}	Energy dissipated in the plate due to plastic flow of the target material
E_{in}	Inertial energy related to displacement of the plate material from the path of the projectile
E_{fric}	Frictional energy dissipated at the sliding interface between the projectile and the target plate material
E_{bulge}	Energy absorbed in unconstrained plastic deformation of the plate material
E_{ben}	Energy absorbed in plastic bending, in front of the penetrating projectile
E_{str}	Energy absorbed in stretching the bulged zone, ahead.

Since T/D ratio is < 1 ($T/D = 0.5$) and also no lip formation is observed on the front-face of the target plate, there is sufficient reason to conclude that, except in the early stages of penetration or perforation, plate material flow, to a large extent, had been in the direction of motion of the projectile. In such a situation, frictional energy can thus be neglected,

DIKSHIT: OBLIQUE IMPACT STUDY IN THIN STEEL PLATE

Table 2. Target behaviour on interaction with projectile

Phenomena	Target hardness	Target thickness	How it looks
Ductile hole formation	Low and medium	Thick $\frac{T}{D} > 1$	
Plugging	High	Thick $\frac{T}{D} < 1$	
Bulging and dishing	Low	Thin $\frac{T}{D} < 1$	
Spalling or (scabbing)	Low and medium	Thick $\frac{T}{D} > 1$	
Front spalling	High	Thick $\frac{T}{D} > 1$	
Front petalling	Low	Thick $\frac{T}{D} > 1$	
Rear petalling	Low	Thin $\frac{T}{D} \ll 1$	
Fragmentation	High	Thick $\frac{T}{D} > 1$	

i.e. $E_{fric} = 0$

Therefore

$$KE_p = E_{pl} + E_{in} + E_{str} + E_{ben}$$

Energy dissipated into the target plate due to the formation of the plug (E_{plug}) may have to be added to the above-mentioned equation; as such a phenomenon may prevail in some cases involving low and medium hardness steel plates at higher velocities. It is to be noted that till 1986, no phenomenological model of cylindrical or cylindro-conical penetration or perforation had been developed for oblique impact⁵.

For advancing further analysis, a large number of projectile-target properties in static and dynamic conditions are required. Critical experimental data could not be obtained due to some technical difficulties involved with the gun. The important information needed to present the analysis includes:

- (a) Residual velocity of the projectile after perforating the plate
- (b) Damage pattern at low velocity ($V < 300$ m/s)
- (c) Plastic zone size and shape.

Thus, the experimental study presented in this paper does not offer theoretical analysis, but provides experimental evidence with regard to protective capability of 10 mm steel armour plate impacted by ogive-shaped steel projectile of 20 mm diameter in the subordnance velocity regime at different obliquities. The paper also provides details of energy absorption modes in a general way. This work is being extended for a T/D ratio > 1 .

5. CONCLUSIONS

An experimental programme was undertaken to evaluate the protective ability of 10 mm thick RHA plate when impacted by a 20 mm diameter steel projectile at 15, 30 and 45° obliquities. The following points have emerged from the study:

10 mm thick RHA plate does not provide protection against 20 mm diameter steel

projectile at 15° angle of attack, even at a low velocity ($V = 300$ m/s).

At 30° angle of attack, the plate provides protection only up to a striking velocity of 340 m/s.

At 45° angle of attack, the 10 mm plate provides full protection against 20 mm diameter steel projectile up to a striking velocity of 530 m/s.

- Normal component for projectile velocity is the main cause of the plate damage at different obliquities.
- At a constant velocity, penetration decreases with increasing obliquity, leading to the increased protective ability of the plate.

ACKNOWLEDGEMENT

The author expresses his gratitude to Shri S.L.N. Acharyulu, the then Director, Defence Metallurgical Research Laboratory (DMRL), Hyderabad, for granting permission to publish this paper. Encouragement provided by Dr P. Rama Rao, Chairman, Atomic Energy Regulatory Board, Government of India, is also sincerely acknowledged.

REFERENCES

1. Corbet, G.G.; Reid, S.R.; and Johnson, W. Impact loading of plates and shells by free - flying projectiles : A review. *Int. J. Impact. Engg.*, 1996, **18**, (2), 141 - 230.
2. Rech, R.F. & Ipson, T.W., Ballistic perforation dynamics. *J. Appl. Mech.*, September 1963.
3. Awerbuch, J.; & Mechanics, A. Approach to projectile penetration *Israel J. Tech.*, 1970, **8**, 375-83.
4. Awerbuch, J., & Bodner, S.R. An investigation of oblique perforation of metallic plates by projectiles. *Experimental Mechanics*, 1977, **17**, 147 - 53.
5. Goldsmith, W. & Finnegan, S.A. Normal and oblique impact of cylindro-conical and

- cylindrical projectiles on metallic plates, *Int. J. Impact Engg.*, 1986, 4, 83.
6. Sundararajan, G. The energy absorbed during the oblique impact of a hardball against ductile target material. *Int. J. Impact Engg.*, 1980, 9 (3) 343-58.
 7. Dikshit, S.N. & Sundararajan, G. Effect of clamping rigidity of the armour on ballistic performance. *Def. Sci. J.*, 1992, 42 (2), 117-20.
 8. Dikshit, S.N. & Sundararajan, G. The penetration of thick steel plates by ogive-shaped projectiles-experiment and analysis. *Int. J. Impact Engg.*, 1992, 12, (3), 373-408.
 9. Hessmann, W. & Wilbeck, J.S. Review of hyper velocity penetration theories. *Int. J. Impact Engg.*, 1987, 5 (1-4), 307-22.
 10. Backman, M.A. & Goldsmith, W. The mechanics of penetration of projectiles into targets. *Int. J. Engg. Sci.*, 1978, 16, 1-99.
 11. Dikshit, S.N. Studies on the ballistic performance of thick armour steel plates, Banaras Hindu University, Varanasi, 1993. PhD Thesis (Unpublished).